Bearings-based cooperative navigation for arbitrary formation topologies

Pedro Mendes
Instituto Superior Técnico
pedro.a.mendes@tencnico.ulisboa.pt

Abstract— **This work compares several cooperative navigation solutions for formations of autonomous vehicles, equipped with depth sensors and capable of taking bearing measurements to their neighbors under a certain measurement topology. Two approaches based on the extended Kalman are described, one centralized and the other decentralized. Additionally, four other Kalman filter implementations based on systems with linear dynamics using artificial measurements are also described, one centralized and the remaining ones decentralized. The presented algorithms were chosen for their simplicity, robustness, and scalability, which are all important design parameters when choosing an observer. Special emphasis was given to algorithms that require minimal communication, since the operating environment might not allow for high-bandwidth and low-latency communication with current technology, as is the case in underwater applications. Additionally, only algorithms that can handle arbitrary measurement topologies were considered, since one of the objectives of this work is to investigate algorithms that are versatile enough to do so. These algorithms were subsequently implemented in a simulation environment and their performance was analyzed. Monte Carlo results were obtained in order to investigate the impact of the measurement topology on the behavior of the algorithms. In particular, the root-mean-squared-error of the obtained estimates and their mean error were investigated.**

I. INTRODUCTION

Advances in technology in the past years have brought increased interest towards the development of autonomous vehicles. Not only do these allow for missions which come at minimal risk for humans, but they also allow for use of cheaper and smaller vehicles, since they do not need to be manned. This makes autonomous vehicles a very captivating technology for activities such as surveillance, scientific exploration, resource gathering, and rescue missions, among others.

Unmanned vehicles (UVs) can be distinguished by their respective fields of application and operating environment (space, water and ground). Unmanned aerial vehicles (UAVs) and autonomous underwater vehicles AUVs are of special interest. The navigation problem for these differs from that of the unmanned ground vehicle (UGV) navigation problem, not only due to the extra spatial dimension, but also due to the fact that their respective operating fluid's momentum will have a much larger effect on the vehicles' kinematics than in the UGV problem.

An essential part of a system of autonomous vehicles is the localization aspect, which is more challenging in underwater applications due to the lack of reliable access to satellite navigation systems. Because of this, underwater localization must be performed via relative measurements and information exchange between agents. Due to the underwater attenuation of the electromagnetic spectrum used for conventional communication, centralized approaches might become impractical due to bandwidth or range restrictions. Thus, there is a need for decentralized navigation algorithms, which scale better with the number of agents and are possibly more robust.

In this work, the problem of decentralized state estimation for an unmanned vehicle formation is considered, whereby the agents attempt to localize themselves and estimate their local fluid velocity through measurements and information exchange with their neighbors. The development of this work led to the publication of [1], in which two of the approaches studied here were analyzed. In addition to these, this work includes approaches based on systems which present linear observation dynamics, from which it is possible to obtain good convergence properties.

A. Related work

Much work has been done on the subject of decentralized navigation. Some approaches, including the ones presented in this work, have their basis on the widely used Kalman filter, which remains a powerful tool when it comes to state estimation in the presence of Gaussian white noise.

In [2], the authors attempt to replicate the centralized Kalman filter by using a communication scheme to distribute all dead-reckoning and measurement information between agents, such that they can all manage a centralized Kalman filter with all the information. This approach does not take advantage of the benefits of decentralization, such as scalability, and requires too much communication between agents, which is not desirable. Other works, such as [3], also attempt to reproduce the centralized filter through bookkeeping strategies. In [4], the authors present a decentralized solution based on the covariance intersection algorithm to build a consistent Kalman filter estimator, guaranteeing that its estimates do not become overconfident, which is important in order to prevent divergence of solutions based on the extended Kalman filter [5]. More recently, [6] presented a decentralized algorithm which approximates the centralized Kalman filter while requiring very limited communication between neighbors and showing good scalability. This algorithm is applied in this work, considering bearing and depth measurements in an extended Kalman filter version of the algorithm, as well as modified version, which uses the definition of an artificial output. The considered system output is based on the work [7], whereby independent observers are designed using a bearing-based artificial output, which guarantees global asymptotic stability in acyclical formations. Another approached based on the Kalman filter for linear time-invariant systems is presented in [8], whereby the authors present a method for computing gain matrices for each agent. This approach is also used in this work by applying the method for computing the gain matrices to artificially constructed position difference measurements.

B. Notation

In this section, the notation adopted throughout this work is defined. Vectors and matrices are represented in bold and their scalar entries are superscripted, such that $\mathbf{v} = (\mathbf{v}^i) \in \mathbb{R}^n$ and $\mathbf{A} = (\mathbf{A}^{ij}) \in \mathbb{R}^{m\times n}$. The identity and zero square matrices of size n are represented as $\mathbf{I}_n$ and $\mathbf{0}_n$, respectively. If the zero matrix is not square, then it is represented as $\mathbf{0}_{m\times n} \in \mathbb{R}^{m\times n}$. The transpose operator is represented by $(\cdot)^T$ and $\mathrm{diag}(\cdot)$ builds a diagonal matrix from the arguments. Additionally, the Kronecker product is denoted by the symbol $\otimes$, such that, for $\mathbf{A} \in \mathbb{R}^{m\times n}$, $\mathbf{B} \in \mathbb{R}^{p\times q}$, one has

$$A \otimes B := \begin{bmatrix} \mathbf{A}^{11}\mathbf{B} & \cdots & \mathbf{A}^{1n}\mathbf{B} \\ \vdots & \ddots & \vdots \\ \mathbf{A}^{m1}\mathbf{B} & \cdots & \mathbf{A}^{mn}\mathbf{B} \end{bmatrix} \in \mathbb{R}^{pm\times qn}.$$

If $\mathcal{S}$ denotes a set, $|\mathcal{S}|$ represents its cardinality, i.e., the number of elements in $\mathcal{S}$.

II. Problem statement

Consider a set of UVs, numbered from 1 to N, operating in a 3D environment such that the movement of each UV in the inertial frame, $\{I\}$, is described by

$$\begin{cases} \dot{\mathbf{p}}_i(t) = \mathbf{R}_i(t)\mathbf{v}_{r_i}(t) + \mathbf{v}_{f_i}(t) \\ \dot{\mathbf{v}}_{f_i}(t) = \mathbf{0}_3 \end{cases},$$

where $\mathbf{p}_i(t) = \begin{bmatrix} \mathbf{p}_i^x(t) & \mathbf{p}_i^y(t) & \mathbf{p}_i^z(t) \end{bmatrix}^T \in \mathbb{R}^3$ represents the position of the i^{th} UV, $\mathbf{R}_i \in SO(3)$ is the rotation matrix that describes the attitude of the agent, transforming coordinates in its body frame to coordinates in the inertial frame, and $\mathbf{v}_{r_i}(t)$ is its local velocity relative to the fluid it is operating in, represented in the UV's body frame. Note that, in practical terms, $\mathbf{v}_{f_i}$ is a function of both time and the position, $\mathbf{p}_i$, of the agent. However, in nominal terms, it is assumed to be constant. In practice, by appropriate tuning of the parameters of the filtering solution, it is possible to estimate slowly time-varying quantities.

Since solutions are usually implemented on a digital computer, the continuous-time kinematics must be discretized, resulting in

$$\begin{cases} \mathbf{p}_i(t_{k+1}) = \mathbf{p}_i(t_k) + T\mathbf{v}_{f_i}(t_k) + \mathbf{u}_i[k] \\ \mathbf{v}_{f_i}(t_{k+1}) = \mathbf{v}_{f_i}(t_k) \end{cases}, \tag{1}$$

where

$$\mathbf{u}_i[k] = \int_{t_k}^{t_{k+1}} \mathbf{R}_i(t)\mathbf{v}_{r_i}(t)dt \tag{2}$$

and T is the sampling time. In state-space form, letting the state of the i^{th} agent be defined as

$$\mathbf{x}_i[k] := \begin{bmatrix} \mathbf{p}_i(t_k) \\ \mathbf{v}_{f_i}(t_k) \end{bmatrix} \in \mathbb{R}^6, \tag{3}$$

and following (1), the motion model of an agent is given by

$$\mathbf{x}_i[k+1] = \mathbf{A}\mathbf{x}_i[k] + \mathbf{B}\mathbf{u}_i[k],$$

where

$$\mathbf{A} := \begin{bmatrix} \mathbf{I}_3 & T\mathbf{I}_3 \\ \mathbf{0}_3 & \mathbf{I}_3 \end{bmatrix} \tag{4}$$

and

$$\mathbf{B} := \begin{bmatrix} \mathbf{I}_3 \\ \mathbf{0}_3 \end{bmatrix}. \tag{5}$$

The UVs are equipped with sensors that enable them to make measurements about themselves, such as depth and attitude measurements; and about their neighbors, such as bearing measurements. In addition to this, they are also capable of some degree of communication between themselves, enabling them to share quantities, such as position estimates, with their neighbors. A major feature of some of the estimators presented in this work is the use of an artificial direction measurement, which is can be constructed from the bearing angles that agent i measures with respect to agent j, θ_{ij} and ϕ_{ij}. These can be used to construct the inertial direction vector from agent i to agent j, $\mathbf{d}_{ij}$, through

$$\begin{aligned} \mathbf{d}_{ij}(t_k) &= \mathbf{R}_i(t_k) \begin{bmatrix} \cos\theta_{ij}(t_k)\cos\phi_{ij}(t_k) \\ \cos\theta_{ij}(t_k)\sin\phi_{ij}(t_k) \\ \sin\theta_{ij}(t_k) \end{bmatrix} \\ &= \frac{\mathbf{p}_j(t_k) - \mathbf{p}_i(t_k)}{||\mathbf{p}_j(t_k) - \mathbf{p}_i(t_k)||}, \end{aligned} \tag{6}$$

where the last equality holds given noiseless attitude and bearing measurements.

At this point, it is assumed that if the j^{th} UV is capable of taking measurements about the i^{th} agent, then there is a bidirectional communication link between the two. The formation's measurement configuration can then be represented with a single directed graph $\mathcal{G} := (\mathcal{V}, \mathcal{E})$, where $\mathcal{V}$ is the set of UVs and $\mathcal{E}$ is the set of directed edges, representing measurement information flow. The j^{th} UV takes measurements about the i^{th} UV if there is a directed edge leaving node i and entering node j, i.e., if there is an edge $e_{ij} = (i, j)$. The neighbor set of the i^{th} UV is then defined as the set of UVs that it takes measurements about, i.e., $\mathcal{N}_i = \{j : (j, i) \in \mathcal{E}\}$. It is also assumed that $\mathcal{V}$ can be further separated into two disjoint subsets, $\mathcal{V}_\mathcal{L}$ and $\mathcal{V}_\mathcal{F}$, such that $\mathcal{V}_\mathcal{L} \cup \mathcal{V}_\mathcal{F} = \mathcal{V}$. The set $\mathcal{V}_\mathcal{L}$ contains the so-called *leader* UVs, which are assumed to able to estimate their position with some accuracy by themselves, and the set $\mathcal{V}_\mathcal{F}$ contains the *follower* UVs, that must estimate their state based on measurements about their neighbors and communication with them.

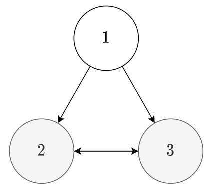

Fig. 1: Example measurement graph.

Example 1: Consider the measurement graph, $\mathcal{G}$, presented in Fig. 1. In this example, the leader set is $\mathcal{V}_{\mathcal{L}} = \{1\}$ and the follower set is $\mathcal{V}_{\mathcal{F}} = \{2, 3\}$, which is graphically represented with grayed out nodes. As per the previous definitions, the 2nd UV takes measurements about and receives information from the 1st and 3rd agents. Likewise for the 3rd UV, which takes measurements about agents 1 and 2, one has $\mathcal{N}_3 = \{1, 2\}$. The neighbor sets of the UVs 1 and 2 are $\mathcal{N}_1 = \emptyset$ and $\mathcal{N}_2 = \{1, 3\}$, respectively.

The decentralized navigation problem addressed in this paper is to estimate the position $\mathbf{p}_i$ of each UV, as well as its local fluid velocity $\mathbf{v}_{f_i}$, constrained by the fact that the agents only have access to local information that they can obtain, be it through measurements or limited communication with their neighbors. In addition to the decentralized navigation approaches presented in this work, centralized solutions are presented as well, in order to establish a baseline for comparison with their decentralized alternatives.

III. Extended Kalman filter solutions

The most straightforward approach to the navigation problem is by using the measurements captured by the UVs directly by employing an extended Kalman filter (EKF), which requires the linearization of the observation model. EKF-based solutions are usually not guaranteed to be globally convergent to the true solution and might require fine tuning of the filter parameters.

A. Centralized extended Kalman filter

While the centralized extended Kalman filter (CEKF) has access to all data, this comes with some serious drawbacks, such as heavy reliance on communication between UVs and lack of scalability. Regardless, they have the potential to give the "best" estimates, and, as such, the CEKF is presented for comparison with its decentralized counterpart.

1) Motion updates: Define the whole state as

$$\mathbf{x}[k] := \begin{bmatrix} \mathbf{x}_1[k] \\ \vdots \\ \mathbf{x}_N[k] \end{bmatrix} \in \mathbb{R}^{6N},$$

where each $\mathbf{x}_i$ is defined as in (3), representing the position and local fluid velocity of each UV. Then, considering $\mathbf{A}$ and $\mathbf{B}$ as defined in (4) and (5), the complete system motion model is given by

$$\mathbf{x}[k+1] = \mathbf{A}_c \mathbf{x}[k] + \mathbf{B}_c \mathbf{u}[k],$$

where

$$\begin{cases} \mathbf{A}_c = \mathbf{I}_N \otimes \mathbf{A} \\ \mathbf{B}_c = \mathbf{I}_N \otimes \mathbf{B} \\ \mathbf{u}[k] = \begin{bmatrix} \mathbf{u}_1[k] \\ \vdots \\ \mathbf{u}_N[k] \end{bmatrix} \end{cases}, \tag{7}$$

with $\mathbf{u}_i[k]$ defined in (2), and $N = |\mathcal{V}|$ is the number of agents. The prediction step for the CEKF is given by

$$\begin{cases} \hat{\mathbf{x}}[k+1|k] = \mathbf{A}_c \hat{\mathbf{x}}[k] + \mathbf{B}_c \mathbf{u}[k] \\ \mathbf{\Sigma}[k+1|k] = \mathbf{A}_c \mathbf{\Sigma}[k|k] \mathbf{A}_c^T + \mathbf{Q}_c \end{cases}, \tag{8}$$

where $\hat{\mathbf{x}}$ and $\mathbf{\Sigma}$ are the state estimate mean and covariance matrix, respectively, and $\mathbf{Q}_c$ is the centralized process noise covariance matrix.

2) Measurement updates: In the following, the discrete-time dependence of the agents is omitted for clarity, unless explicitly needed. Let $\mathbf{y}_i = \mathbf{h}_i(\mathbf{x})$ be a measurement taken by an UV with index i, and let the complete measurement vector, $\mathbf{y}$, be the concatenation of all the individual measurement vectors, as in

$$\mathbf{y} = \mathbf{h}(\mathbf{x}) = \begin{bmatrix} \mathbf{h}_1(\mathbf{x}) \\ \vdots \\ \mathbf{h}_N(\mathbf{x}) \end{bmatrix}.$$

In order to perform the update step of the CEKF, the Jacobian of the measurement model must be computed according to

$$\mathbf{J}(\mathbf{x}) = \begin{bmatrix} \partial \mathbf{h}_1 / \partial \mathbf{x} \\ \vdots \\ \partial \mathbf{h}_N / \partial \mathbf{x} \end{bmatrix} = \begin{bmatrix} \partial \mathbf{h}_1 / \partial \mathbf{x}_1 & \cdots & \partial \mathbf{h}_1 / \partial \mathbf{x}_N \\ \vdots & \ddots & \vdots \\ \partial \mathbf{h}_N / \partial \mathbf{x}_1 & \cdots & \partial \mathbf{h}_N / \partial \mathbf{x}_N \end{bmatrix}. \tag{9}$$

Since the real state is unknown, the Jacobian, $\mathbf{J} = \mathbf{J}(\mathbf{x})$, is approximated by $\hat{\mathbf{J}} = \mathbf{J}(\hat{\mathbf{x}})$, hence one of the reasons why a good enough initial state estimate is necessary.

Since EKF-based approaches allow for arbitrary measurement models, the general update equations are presented here, and some specific measurement models are described in the following section. Upon receiving measurements, the CEKF update equations are given by

$$\begin{cases} \hat{\mathbf{x}}[k+1|k+1] = \hat{\mathbf{x}}[k+1|k] + \mathbf{K} \left(\mathbf{y}[k+1] - \hat{\mathbf{y}}[k+1] \right) \\ \mathbf{\Sigma}[k+1|k+1] = \left(\mathbf{I}_{6N} - \mathbf{K} \hat{\mathbf{J}} \right) \mathbf{\Sigma}[k+1|k] \end{cases},$$

where $\mathbf{K} = \mathbf{\Sigma}[k+1|k] \hat{\mathbf{J}}^T \left(\hat{\mathbf{J}} \mathbf{\Sigma}[k+1|k] \hat{\mathbf{J}}^T + \mathbf{R}_c \right)^{-1}$ is the Kalman gain, with $\hat{\mathbf{J}}$ evaluated using the predicted estimate, $\hat{\mathbf{x}}[k+1|k]$, and $\mathbf{R}_c$ is the centralized measurement vector noise covariance matrix. Lastly, $\hat{\mathbf{y}}[k+1] = \mathbf{h}(\hat{\mathbf{x}}[k+1|k])$ is the expected value of the measurement vector, given the current state estimate.

3) Measurement models: Some common measurement models will now be introduced. In particular, models for position, depth, and bearing measurements are presented. For ease of representation, the explicit discrete-time dependence is omitted unless explicitly necessary.

If the UV making a measurement has direct access to position measurements $\mathbf{y}_i = \mathbf{h}_i(\mathbf{x}) = \mathbf{p}_i(t_k)$, its relevant part in (9) is given by $\partial\mathbf{h}_i/\partial\mathbf{x} = \begin{bmatrix}\cdots & \mathbf{I}_3 & \mathbf{0}_3 & \cdots\end{bmatrix}$, where i is the index of the measuring agent and $\mathbf{I}_3$ occupies the columns corresponding to $\mathbf{p}_i$ in the complete state vector. If, on the other hand, the i^{th} UV takes bearing measurements about UVs in its neighbor set, which, for simplicity, is assumed to be $\mathcal{N}_i = \{1, \ldots, |\mathcal{N}_i|\}$, in addition to a depth measurement about itself, $z_i(t_k) = \mathbf{p}_i^z(t_k)$, the measurement model is given by

$$\mathbf{h}_i(\mathbf{x}) = \begin{bmatrix}\mathbf{h}_{i1}\\ \vdots \\ \mathbf{h}_{i|\mathcal{N}_i|}\\ \mathbf{p}_i^z\end{bmatrix},$$

where

$$\begin{aligned}\mathbf{h}_{ij}(\mathbf{x}) = \mathbf{h}_b(\mathbf{p}_i, \mathbf{p}_j) &= \begin{bmatrix}{}^{\mathcal{I}}\theta(\mathbf{p}_i, \mathbf{p}_j)\\ {}^{\mathcal{I}}\phi(\mathbf{p}_i, \mathbf{p}_j)\end{bmatrix}\\ &= \begin{bmatrix}\operatorname{atan2}\left(\mathbf{p}_j^z - \mathbf{p}_i^z, \sqrt{(\mathbf{p}_j^x - \mathbf{p}_i^x)^2 + (\mathbf{p}_j^y - \mathbf{p}_i^y)^2}\right)\\ \operatorname{atan2}\left(\mathbf{p}_j^y - \mathbf{p}_i^y, \mathbf{p}_j^x - \mathbf{p}_i^x\right)\end{bmatrix},\end{aligned}$$

and the angles ${}^{\mathcal{I}}\theta$ and ${}^{\mathcal{I}}\phi$ are represented in the inertial frame. Bearing measurements are measured in the UV's body frame. However, the UVs measure their orientation and, as such, can rotate the bearing measurement so that it is represented in $\{I\}$. The Jacobian for the model $\mathbf{h}_i$ is given by

$$\frac{\partial\mathbf{h}_i}{\partial\mathbf{x}}(\mathbf{x}) = \begin{bmatrix}\partial\mathbf{h}_{i1}/\partial\mathbf{x}\\ \vdots \\ \partial\mathbf{h}_{i|\mathcal{N}_i|}/\partial\mathbf{x}\\ \mathbf{C}_z\end{bmatrix},$$

where

$$\frac{\partial\mathbf{h}_{ij}}{\partial\mathbf{x}}(\mathbf{x}) = \begin{bmatrix}\cdots & \mathbf{J}_{b_i}(\mathbf{x}) & \cdots & \mathbf{J}_{b_j}(\mathbf{x}) & \cdots\end{bmatrix},$$

with $\mathbf{J}_{b_i} := \partial\mathbf{h}_b/\partial\mathbf{x}_i$ and $\mathbf{J}_{b_j} := \partial\mathbf{h}_b/\partial\mathbf{x}_j$, and $\mathbf{C}_z \in \mathbb{R}^{1\times 6N}$ is such that all entries are zero except the one corresponding to $\mathbf{p}_i^z$ in the entire state vector. The explicit expression of the bearing model Jacobian is omitted for brevity.

B. Decentralized extended Kalman filter

In this section, an implementation of the solution presented in [6] is described for depth and bearing measurements, which will be labeled in this work as decentralized extended Kalman filter (DEKF). This asynchronous approach is completely decentralized and relies only on local communication between agents.

1) Motion model: Consider the state of the i^{th} agent, $\mathbf{x}_i$, defined as in (3), and denote its filtered estimate and covariance by $\hat{\mathbf{x}}_i$ and $\hat{\mathbf{\Sigma}}_{ii}$, respectively. Note that the DEKF approximates the CEKF, thus the covariances of each agent and their cross-covariances to other agents will not be exact, hence the chosen hat notation. Consider also the decomposition of the cross-covariance between agents i and j, $\hat{\mathbf{\Sigma}}_{ij}$, such that

$$\hat{\mathbf{\Sigma}}_{ij}[k] = \hat{\mathbf{\Phi}}_{ij}[k]\hat{\mathbf{\Phi}}_{ji}^T[k].$$

Let each agent carry its estimated belief, $\mathcal{B}_i := \{\hat{\mathbf{x}}_i, \hat{\mathbf{\Sigma}}_{ii}\}$, and cross-covariance factor, $\hat{\mathbf{\Phi}}_{ij}$, between itself and other agents it has knowledge of, i.e. $\hat{\mathbf{\Phi}}_{ij}$ for all $j \in \mathcal{N}_i$. The corresponding CEKF prediction equations for agent i, which account for its motion, are given by

$$\begin{cases}\hat{\mathbf{x}}_i[k+1|k] = \mathbf{A}\hat{\mathbf{x}}_i[k|k] + \mathbf{B}\mathbf{u}_i[k]\\ \mathbf{\Sigma}_{ii}[k+1|k] = \mathbf{A}\mathbf{\Sigma}_{ii}[k|k]\mathbf{A}^T + \mathbf{Q}_i\\ \mathbf{\Sigma}_{ij}[k+1|k] = \mathbf{A}\mathbf{\Sigma}_{ij}[k|k]\end{cases}, \tag{10}$$

leaving the remaining terms $\hat{\mathbf{x}}_j, \mathbf{\Sigma}_{jj}$ for all $j \neq i$, unchanged. So, if UV i updates its cross-covariance factor to another UV j through

$$\hat{\mathbf{\Phi}}_{ij}[k+1|k] = \mathbf{A}\hat{\mathbf{\Phi}}_{ij}[k|k]\ \forall j \in \mathcal{N}_i \tag{11}$$

when performing prediction steps, when they meet, their reconstructed cross-covariance is given by

$$\begin{aligned}\hat{\mathbf{\Sigma}}_{ij}[k+1|k] &= \mathbf{A}\hat{\mathbf{\Phi}}_{ij}[k|k]\hat{\mathbf{\Phi}}_{ji}[k|k]^T\\ &= \mathbf{A}\hat{\mathbf{\Sigma}}_{ij}[k|k]\\ &= \mathbf{\Sigma}_{ij}[k+1|k],\end{aligned}$$

if it holds that $\hat{\mathbf{\Sigma}}_{ij}[k|k] = \mathbf{\Sigma}_{ij}[k|k]$. In general, $\hat{\mathbf{\Sigma}}_{ij}[k|k] \neq \mathbf{\Sigma}_{ij}[k|k]$, however, what is important is that, since all terms are available, the prediction step of the CEKF can be reproduced exactly at each agent in a decentralized way while requiring no communication, thus resulting in no loss of estimation capabilities with respect to this step. All UVs then predict their beliefs and cross-covariance factors to other agents according to (10) and (11), substituting $\mathbf{x}_i$ and $\mathbf{\Sigma}_{ii}$ by their estimated state and covariance matrix, $\hat{\mathbf{x}}_i$ and $\hat{\mathbf{\Sigma}}_{ii}$.

2) Observation model: While all the measurements are available simultaneously for computation of the update step in the CEKF, the DEKF is asynchronous and, as such, only one measurement vector is considered at a time. In a centralized approach, this would be equivalent to considering an observation model containing only one measurement at a time and performing several updates at each time step.

Consider that a leader UV with index i takes a measurement, $\mathbf{y}_i$, of its position. Dropping the explicit discrete-time dependence, the measurement model for this agent is given by

$$\mathbf{h}(\mathbf{x}_i) = \begin{bmatrix}\mathbf{I}_3 & \mathbf{0}_3\end{bmatrix}\mathbf{x}_i = \mathbf{C}_i\mathbf{x}_i.$$

Since this equation only involves the measuring agent, the estimated belief and cross-covariance factors to other agents are updated according to

$$\begin{cases}\hat{\mathbf{x}}_i[k+1|k+1] = \hat{\mathbf{x}}_i[k+1|k]\\ \qquad\qquad + \mathbf{K}_i(\mathbf{y}_i[k+1] - \hat{\mathbf{y}}_i[k+1])\\ \hat{\mathbf{\Sigma}}_{ii}[k+1|k+1] = (\mathbf{I}_6 - \mathbf{K}_i\mathbf{C}_i)\,\hat{\mathbf{\Sigma}}_{ii}[k+1|k]\\ \hat{\mathbf{\Phi}}_{ij}[k+1|k+1] = (\mathbf{I}_6 - \mathbf{K}_i\mathbf{C}_i)\,\hat{\mathbf{\Phi}}_{ij}[k+1|k]\end{cases}, \tag{12}$$

where $\hat{\mathbf{y}}_i[k+1] = \mathbf{h}(\hat{\mathbf{x}}_i[k+1|k])$ is the expected measurement vector, $\mathbf{K}_i$ is the Kalman gain, given by

$$\mathbf{K}_i = \hat{\boldsymbol{\Sigma}}_{ii}[k+1|k]\mathbf{C}_i^T \left(\mathbf{C}_i\hat{\boldsymbol{\Sigma}}_{ii}[k+1|k]\mathbf{C}_i^T + \mathbf{R}_i\right)^{-1},$$

and $\mathbf{R}_i$ is the measurement noise covariance matrix. Note that the last equation of (12) should be performed for all agents that UV i has knowledge of. In a centralized Kalman filter, measurements taken by an agent also affect the state of all agents that are correlated with it through previous measurements. However, in order to prevent excessive communication, the estimated beliefs of other agents are left unchanged.

Consider now the case where a follower UV with index i takes a bearing measurement about another UV with index j and a depth measurement about itself. Let $\hat{\mathbf{x}}_a$ be the joint estimate of the states, $\mathbf{x}_i$ and $\mathbf{x}_j$, and $\hat{\boldsymbol{\Sigma}}_{aa}$ its estimated covariance, such that

$$\hat{\mathbf{x}}_a[k] := \begin{bmatrix}\hat{\mathbf{x}}_i\\ \hat{\mathbf{x}}_j\end{bmatrix}, \qquad \hat{\boldsymbol{\Sigma}}_{aa} := \begin{bmatrix}\hat{\boldsymbol{\Sigma}}_{ii} & \hat{\boldsymbol{\Sigma}}_{ij}\\ \hat{\boldsymbol{\Sigma}}_{ji} & \hat{\boldsymbol{\Sigma}}_{jj}\end{bmatrix}.$$

The update equations for the joint system are given by

$$\begin{cases}\hat{\mathbf{x}}_a[k+1|k+1] = \hat{\mathbf{x}}_a[k+1|k] \\ \qquad\qquad + \mathbf{K}_a(\mathbf{y}_i[k+1] - \hat{\mathbf{y}}_i[k+1]) \\ \hat{\boldsymbol{\Sigma}}_{aa}[k+1|k+1] = \left(\mathbf{I}_6 - \mathbf{K}_a\hat{\mathbf{J}}_a\right)\hat{\boldsymbol{\Sigma}}_{aa}[k+1|k]\end{cases}, \quad (13)$$

where $\mathbf{y}_i[k+1]$ is the concatenation of the bearing measurement to another UV with the captured depth measurement, $\hat{\mathbf{y}}_i[k+1]$ is its expected value, $\hat{\mathbf{J}}_a = \begin{bmatrix}\mathbf{J}_{f_i}(\hat{\mathbf{x}}_i, \hat{\mathbf{x}}_j) & \mathbf{J}_{f_j}(\hat{\mathbf{x}}_i, \hat{\mathbf{x}}_j)\end{bmatrix}$ is the Jacobian matrix of the joint system's measurement model computed using the predicted state estimates, $\hat{\mathbf{x}}_i[k+1|k]$ and $\hat{\mathbf{x}}_j[k+1|k]$, with $\mathbf{J}_{f_i}$ and $\mathbf{J}_{f_j}$ defined as

$$\begin{cases}\mathbf{J}_{f_i}(\mathbf{x}_i, \mathbf{x}_j) & := \begin{bmatrix}\mathbf{J}_{b_i}(\mathbf{x}_i, \mathbf{x}_j)\\ \mathbf{C}_z\end{bmatrix}\\ \mathbf{J}_{f_j}(\mathbf{x}_i, \mathbf{x}_j) & := \begin{bmatrix}\mathbf{J}_{b_j}(\mathbf{x}_i, \mathbf{x}_j)\\ \mathbf{0}_{1\times 6}\end{bmatrix}\end{cases},$$

and $\mathbf{K}_a$ is the Kalman gain, given by

$$\mathbf{K}_a = \hat{\boldsymbol{\Sigma}}_{aa}[k+1|k]\hat{\mathbf{J}}_a^T \left(\hat{\mathbf{J}}_a\hat{\boldsymbol{\Sigma}}_{aa}[k+1|k]\hat{\mathbf{J}}_a^T + \mathbf{R}_i\right)^{-1},$$

where $\mathbf{R}_i$ is the measurement noise covariance matrix. These quantities can be computed locally at the measuring agent, requiring only that UV j transmits its estimated belief, $\mathcal{B}_j$, and its cross-covariance factor to agent i, $\hat{\boldsymbol{\Phi}}_{ji}$. UV i is then responsible for reconstructing the joint system's belief and performing the joint update equations. It then communicates to UV j its updated belief, obtained from the entries of $\hat{\mathbf{x}}_a[k+1|k+1]$ and $\hat{\boldsymbol{\Sigma}}_{aa}[k+1|k+1]$. In order not to double-count information, the cross-covariance between agents i and j must be distributed correctly. Since the decomposition of the cross-covariance between agents can be done in any way, it can be agreed beforehand, as done in [6], that upon receiving updated estimates, agent j sets its cross-covariance factor to UV i as the identity matrix, i.e. $\hat{\boldsymbol{\Phi}}_{ji}[k+1|k+1] = \mathbf{I}_6$, and UV i sets

$$\hat{\boldsymbol{\Phi}}_{ij}[k+1|k+1] = \hat{\boldsymbol{\Sigma}}_{ij}[k+1|k+1], \quad (14)$$

where $\hat{\boldsymbol{\Sigma}}_{ij}[k+1|k+1]$ can be obtained from the updated joint state covariance matrix, $\hat{\boldsymbol{\Sigma}}_{aa}[k+1|k+1]$. This way, the cross-covariance between these two agents is preserved, since $\hat{\boldsymbol{\Phi}}_{ij}[k+1|k+1]\mathbf{I}_6^T = \hat{\boldsymbol{\Sigma}}_{ij}[k+1|k+1]$, and there is no need for communicating to agent j a new cross-covariance factor. As before, in order to prevent communication between participating and non-participating agents, the state and covariance estimates of the latter are left unchanged.

The only terms that still need to tracked are the cross-covariance factors between participating and non-participating agents. This is stated to be the main contribution of the work in [6] and, as such, only the main result is presented here. The interested reader is referred to the original work for details. The last update equation performed by participating agents is

$$\hat{\boldsymbol{\Phi}}_{il}[k+1|k+1] = \hat{\boldsymbol{\Sigma}}_{ii}[k+1|k+1]\hat{\boldsymbol{\Sigma}}_{ii}^{-1}[k+1|k]\hat{\boldsymbol{\Phi}}_{il}[k+1|k], \quad (15)$$

where i represents the index of participating UVs and l the index of non-participating agents. Note that both participating agents should perform the update (15).

To summarize, updates performed by leader UVs when they take a measurement of their position are performed using (12). When an agent with index i takes a bearing measurement about UV with index j, the updates are done using (13), (14), and (15), with UV j setting $\hat{\boldsymbol{\Phi}}_{ji}[k+1|k+1] = \mathbf{I}_6$ upon receiving its updated belief, and performing (15) locally as well.

IV. Artificial measurement solutions

An alternative to EKF-based filters is to construct artificial outputs such that the measurement model becomes linear, and then use this model to build an observer. With this approach, better convergence properties can be achieved, increasing the time-efficiency of missions since an initial setup process is not required.

A. Independently interconnected Kalman filters

In this section, the approach considered in [7] is presented. Briefly, is based on constructing observers which present globally convergent error dynamics for each agent, and interconnecting them by using their estimates as "true" information, which is fed to the other observers. Even though it keeps no cross-measurement information is kept between agents and each agent's estimate is taken as true information by other agents, this estimator achieves the worst performance out of the considered ones, though it does achieve globally convergent dynamics, provided that each agent's observer is globally observable, and the information flow is unidirectional, as is the case for tiered formations [7], [10].

The prediction and update equations for each agent's observer follow the general Kalman filter dynamics. Letting

$\hat{\mathbf{x}}_i$ and $\mathbf{\Sigma}_{ii}$ be the state estimate and covariance of the i^{th} UV, respectively, the prediction step equations are given by

$$\begin{cases} \hat{\mathbf{x}}_i[k+1|k] = \mathbf{A}\hat{\mathbf{x}}[k|k] + \mathbf{B}\mathbf{u}_i[k] \\ \mathbf{\Sigma}_{ii}[k+1|k] = \mathbf{A}\mathbf{\Sigma}_{ii}[k|k]\mathbf{A}^T + \mathbf{Q}_i \end{cases},$$

where $\mathbf{Q}_i$ is the process noise covariance matrix of the agent. Likewise, the update equations are

$$\begin{cases} \hat{\mathbf{x}}_i[k+1|k+1] = \hat{\mathbf{x}}_i[k+1|k] \\ \qquad\qquad + \mathbf{K}_i(\mathbf{y}_i[k+1] - \mathbf{C}_i\hat{\mathbf{x}}_i[k+1|k]) \\ \mathbf{\Sigma}_{ii}[k+1|k+1] = (\mathbf{I}_6 - \mathbf{K}_i\mathbf{C}_i)\,\mathbf{\Sigma}_{ii}[k+1|k] \end{cases},$$

where $\mathbf{C}_i$ is the observation matrix to be described in the following, $\mathbf{y}_i[k+1]$ is the observation vector, constructed using measurements obtained at time $t = t_{k+1}$, and $\mathbf{K}_i$ is the Kalman gain.

Assuming that the i^{th} UV is a leader, then it has direct access to position measurements, such that $\mathbf{y}_i[k+1]$ is its position measurement vector, and $\mathbf{C}_i = \begin{bmatrix}\mathbf{I}_3 & \mathbf{0}_3\end{bmatrix}$. If, instead, the i^{th} agent is a follower UV which successfully obtains bearing measurements about its neighbors, $j \in \mathcal{N}_i$, and its depth, it then has access to $z_i = \mathbf{p}_i^z(t_{k+1})$ and $\mathbf{d}_{ij}(t_{k+1})$ for all $j \in \mathcal{N}_i$, computed from the obtained bearing angles, θ_{ij} and ϕ_{ij}, according to (6). In the following, it is assumed, for ease of representation and without loss of generality, that $\mathcal{N}_i = \{1, \ldots, |\mathcal{N}_i|\}$.

Upon building the direction vector, the projection matrix,

$$\mathbf{D}_{ij}(t_k) := \mathbf{d}_{ij}(t_k)\mathbf{d}_{ij}^T(t_k), \tag{16}$$

and its orthogonal complement,

$$\bar{\mathbf{D}}_{ij}(t_k) := \mathbf{I}_3 - \mathbf{d}_{ij}(t_k)\mathbf{d}_{ij}^T(t_k), \tag{17}$$

are constructed and the following equality holds, $\bar{\mathbf{D}}_{ij}(t_k)\mathbf{p}_i(t_k) = \bar{\mathbf{D}}_{ij}(t_k)\mathbf{p}_j(t_k)$. Since the true positions of the neighboring UVs are unknown, the observation vector of the i^{th} UV, considering also its depth measurement, is defined as

$$\mathbf{y}_i[k+1] := \begin{bmatrix} \bar{\mathbf{D}}_{i1}(t_{k+1})\hat{\mathbf{p}}_1(t_{k+1}|t_k) \\ \vdots \\ \bar{\mathbf{D}}_{i|\mathcal{N}_i|}(t_{k+1})\hat{\mathbf{p}}_{|\mathcal{N}_i|}(t_{k+1}|t_k) \\ z_i(t_{k+1}) \end{bmatrix},$$

where $\hat{\mathbf{p}}_j(t_{k+1}|t_k)$ is the predicted position estimate of the j^{th} agent, extracted from $\hat{\mathbf{x}}_j[k+1|k]$, and z_i is the depth measurement obtained by the i^{th} agent. Likewise, the observation matrix is defined as

$$\mathbf{C}_i := \begin{bmatrix} \bar{\mathbf{D}}_{i1}(t_{k+1}) & \mathbf{0}_3 \\ \vdots & \\ \bar{\mathbf{D}}_{i|\mathcal{N}_i|}(t_{k+1}) & \mathbf{0}_3 \\ \mathbf{e}_z & \mathbf{0}_{1\times 3} \end{bmatrix},$$

where $\mathbf{e}_z = \begin{bmatrix}0 & 0 & 1\end{bmatrix}$.

In [7], an observer such as this one is considered for the case of acyclical formations, where it is shown that it exhibits globally exponentially stable error dynamics, provided that the leader agents also present this kind of error dynamics. If cycles are introduced into the measurement graph, there will be a reintroduction of the estimation errors into some of the agents, which raises some questions about the convergence of the proposed observer. The performance of this filter under a cyclical measurement topology was analyzed via Monte Carlo simulations and some of the results are presented in Section V.

B. Centralized observer

The centralized version of the observers based on bearing and depth measurements is presented in this section. Let the state of the centralized system be defined as

$$\mathbf{x}[k] := \begin{bmatrix} \mathbf{x}_1[k] \\ \vdots \\ \mathbf{x}_N[k] \end{bmatrix} \in \mathbb{R}^{6N}$$

and let $\hat{\mathbf{x}}$ and $\mathbf{\Sigma}$ be its state estimate and covariance matrix, respectively. The motion model of this approach is the same as that of the CEKF, i.e., upon receiving the control signals, the agents' estimates are predicted according to (8). Let $\mathbf{y}$ and $\mathbf{C}_c$ be the complete measurement vector and centralized observation matrix, respectively, such that $\mathbf{y}[k] = \mathbf{C}_c\mathbf{x}[k]$. Let $\mathbf{y}$ be composed of individual agent measurement vectors, such that

$$\mathbf{y} := \begin{bmatrix} \mathbf{y}_1 \\ \vdots \\ \mathbf{y}_N \end{bmatrix}, \qquad \mathbf{C}_c := \begin{bmatrix} \mathbf{C}_1 \\ \vdots \\ \mathbf{C}_N \end{bmatrix}$$

where $\mathbf{y}_i$ is the measurement vector captured by agent i, and $\mathbf{C}_i$ is its measurement model. For the case of leader agents, $\mathbf{y}_i$ is a position measurement and $\mathbf{C}_i = \begin{bmatrix}\cdots & \mathbf{I}_3 & \mathbf{0}_3 & \cdots\end{bmatrix}$. As for follower UVs, considering the relationship presented in [7], $\bar{\mathbf{D}}_{ij}(t_k)(\mathbf{p}_i(t_k) - \mathbf{p}_j(t_k)) = \mathbf{0}_{3\times 1}$, and that the UV has access to depth measurements, the measurement vector, at time $t = t_{k+1}$ is then given by

$$\mathbf{y}_i[k+1] = \begin{bmatrix} \mathbf{0}_{3|\mathcal{N}_i|\times 1} \\ z_i(t_{k+1}) \end{bmatrix},$$

where z_i is the depth measurement. Each $\mathbf{C}_i$ relates the measurements captured by the i^{th} agent with the total state vector using the orthogonal complement of the bearing projection matrix and depth information, such that $\mathbf{y}_i[k] = \mathbf{C}_i\mathbf{x}[k]$. The total state estimate is then corrected according to the standard Kalman filter update equations using the centralized observation matrix, $\mathbf{C}_c$.

C. Decentralized observer

Similarly to the DEKF, each agent carries its own estimated belief, $\mathcal{B}_i = \{\hat{\mathbf{x}}_i, \hat{\mathbf{\Sigma}}_{ii}\}$, and cross-covariance factors to other UVs, $\hat{\mathbf{\Phi}}_{ij}$. The prediction equations for these quantities are performed as in the DEKF. In fact, the only difference between these two approaches is the update step, which is not restricted to pairwise communication and uses the projection matrix (17) introduced in [7].

The update equations for leader agents are the exact same as in the DEKF approach, including the cross-covariance factor updates. On the other hand, let a follower agent with index i take bearing measurements about its neighbors, which will be assumed, without loss of generality, to have indices $j \in \mathcal{N}_i = \{1, \dots, |\mathcal{N}_i|\}$, and a depth measurement about itself. Since $\bar{\mathbf{D}}_{ij}(t_k)(\mathbf{p}_i(t_k) - \mathbf{p}_j(t_k)) = \mathbf{0}_{3\times1}$, then, considering the joint state vector $\mathbf{x}_a[k] := \begin{bmatrix}\mathbf{x}_i^T[k] & \mathbf{x}_1^T[k] & \cdots & \mathbf{x}_{|\mathcal{N}_i|}^T[k]\end{bmatrix}^T$ where $\mathbf{x}_i$ is the state of the measuring agent, one has

$$\mathbf{y}_a[k+1] := \begin{bmatrix}\mathbf{0}_{3\times|\mathcal{N}_i|} \\ z_i(t_{k+1})\end{bmatrix} = \mathbf{C}_a \mathbf{x}_a[k+1],$$

where $\mathbf{C}_a$ establishes constraints between the states, using $\bar{\mathbf{D}}_{ij}$, and z_i is the depth measurement of the measuring agent. Note that the matrices $\bar{\mathbf{D}}_{ij}$ are, again, computed using the quantities obtained at time $t = t_{k+1}$, such that, when computing the update equations, one has $\bar{\mathbf{D}}_{ij} = \bar{\mathbf{D}}_{ij}(t_{k+1})$.

Let the estimate of the joint system's state, composed of the UVs participating in the measurement of agent i, be denoted as $\hat{\mathbf{x}}_a$, and its associated covariance matrix estimate as

$$\hat{\boldsymbol{\Sigma}}_{aa} = \begin{bmatrix} \hat{\boldsymbol{\Sigma}}_{ii} & \hat{\boldsymbol{\Sigma}}_{i1} & \cdots & \hat{\boldsymbol{\Sigma}}_{i|\mathcal{N}_i|} \\ \hat{\boldsymbol{\Sigma}}_{1i} & \hat{\boldsymbol{\Sigma}}_{11} & \cdots & \hat{\boldsymbol{\Sigma}}_{1|\mathcal{N}_i|} \\ \vdots & \vdots & \ddots & \vdots \\ \hat{\boldsymbol{\Sigma}}_{|\mathcal{N}_i|i} & \hat{\boldsymbol{\Sigma}}_{|\mathcal{N}_i|1} & \cdots & \hat{\boldsymbol{\Sigma}}_{|\mathcal{N}_i||\mathcal{N}_i|} \end{bmatrix}, \qquad (18)$$

where the discrete-time dependence was also dropped for readability. In order to reduce the required amount of communication, the cross-covariance terms between the neighbors of UV i can be ignored, such that

$$\hat{\boldsymbol{\Sigma}}_{aa} \approx \begin{bmatrix} \hat{\boldsymbol{\Sigma}}_{ii} & \hat{\boldsymbol{\Sigma}}_{i1} & \cdots & \hat{\boldsymbol{\Sigma}}_{i|\mathcal{N}_i|} \\ \hat{\boldsymbol{\Sigma}}_{1i} & \hat{\boldsymbol{\Sigma}}_{11} & \cdots & \mathbf{0}_{3\times3} \\ \vdots & \vdots & \ddots & \vdots \\ \hat{\boldsymbol{\Sigma}}_{|\mathcal{N}_i|i} & \mathbf{0}_{3\times3} & \cdots & \hat{\boldsymbol{\Sigma}}_{|\mathcal{N}_i||\mathcal{N}_i|} \end{bmatrix}.$$

The cross-covariance terms $\hat{\boldsymbol{\Sigma}}_{jk}$, for $j, k \in \mathcal{N}_i$, can be obtained from the cross-covariance factors that the participating agents j and k carry, by letting them communicate these quantities to agent i, which can then reconstruct the cross-covariance term and place it into $\hat{\boldsymbol{\Sigma}}_{aa}$. For follower UVs, the Kalman gain is computed for the joint system using the reconstructed covariance matrix, such that

$$\mathbf{K}_a = \hat{\boldsymbol{\Sigma}}_{aa}[k+1|k]\mathbf{C}_a^T \left(\mathbf{C}_a \hat{\boldsymbol{\Sigma}}_{aa}[k+1|k]\mathbf{C}_a^T + \mathbf{R}_i\right)^{-1},$$

where $\mathbf{R}_i$ is a compatible measurement noise covariance matrix. The new beliefs are then computed using the standard Kalman filter update equations and then communicated to the participating agents. In turn, these agents update their cross-covariance factors to non-participating ones according to the approximation presented in [6], i.e.,

$$\hat{\boldsymbol{\Phi}}_{ik}[k+1|k+1] = \hat{\boldsymbol{\Sigma}}_{ii}[k+1|k+1]\hat{\boldsymbol{\Sigma}}_{ii}^{-1}[k+1|k]\hat{\boldsymbol{\Phi}}_{ik}[k+1|k],$$

for every non-participating agent with index k that they have knowledge of. In case the full covariance matrix was used, the new cross-covariance terms between the participating agents can be factorized and distributed in a way that does not double-count information. A possible rule for distributing the cross-covariance terms could be, for example

$$\hat{\boldsymbol{\Phi}}_{ij}[k+1|k+1] = \begin{cases} \hat{\boldsymbol{\Sigma}}_{ij}[k+1] & \text{if } i < j \\ \mathbf{I}_6 & \text{if } i > j \end{cases},$$

though it is not necessarily the one which minimizes the amount of communication.

D. Static-gain decentralized observer

In this section, a technique for computing steady-state observer gains for agents that can acquire relative position measurements to their neighbors, presented in [8], is briefly described. Local observers for each follower agent are then designed, coupling these gains with an artificial relative position output built from bearing measurements and depth differences between agents.

All agents predict their estimate according to the standard state prediction equation

$$\hat{\mathbf{x}}_i[k+1|k] = \mathbf{A}\hat{\mathbf{x}}[k|k] + \mathbf{B}\mathbf{u}[k],$$

where $\mathbf{A}$, $\mathbf{B}$, and $\mathbf{u}[k]$ are defined as in (4), (5), and (2), respectively. Upon taking measurements and predicting its state, the i^{th} agent updates its estimate according to

$$\hat{\mathbf{x}}_i[k+1|k+1] = \begin{cases} \hat{\mathbf{x}}_i[k+1|k] + \mathbf{K}_i(\mathbf{y}_i[k+1] - \hat{\mathbf{x}}_i[k+1|k]) & \text{if } i \in \mathcal{V}_L \\ \hat{\mathbf{x}}_i[k+1|k] + \mathbf{K}_i(\mathbf{m}_i[k+1] - \Delta\hat{\mathbf{x}}[k+1|k]) & \text{if } i \in \mathcal{V}_F \end{cases},$$

where

$$\Delta\hat{\mathbf{x}} = \begin{bmatrix} \hat{\mathbf{x}}_i[k+1|k] - \hat{\mathbf{x}}_1[k+1|k] \\ \vdots \\ \hat{\mathbf{x}}_i[k+1|k] - \hat{\mathbf{x}}_{|\mathcal{N}_i|}[k+1|k] \\ \hat{\mathbf{p}}_i^z(t_{k+1}|t_k) \end{bmatrix},$$

$\mathbf{y}_i[k+1]$ is an absolute position measurement, and $\mathbf{m}_i[k+1]$ is a vector containing the captured depth measurement and relative position measurements between the measuring agent and its neighbors, assumed to be $\mathcal{N}_i = \{1, \dots, |\mathcal{N}_i|\}$. The formation gains, $\mathbf{K}_i$, are computed by propagating the centralized system's covariance prediction and update equations using a gain matrix computed subject to a certain sparsity constraint, which, in this case, constrains the total system gain matrix, $\mathbf{K}$, to be block diagonal. Upon computing the formation gains, each block of $\mathbf{K}$ is extracted and set as $\mathbf{K}_i$ accordingly.

The centralized system's motion model is identical to that of the CEKF, such that $\mathbf{A}_c = \mathbf{I}_N \otimes \mathbf{A}$. As for the observation model, whereas leader agents can capture measurements of their own position, follower agents are assumed to capture relative position and depth measurements, that is

$$\mathbf{m}_i[k+1] = \begin{bmatrix} \mathbf{p}_i(t_{k+1}) - \mathbf{p}_1(t_{k+1}) \\ \vdots \\ \mathbf{p}_i(t_{k+1}) - \mathbf{p}_{|\mathcal{N}_i|}(t_{k+1}) \\ z_i(t_{k+1}) \end{bmatrix}.$$

Let $\mathbf{C}_c$ be centralized system's observation matrix, containing matrices $\mathbf{C}_L = \begin{bmatrix}\mathbf{I}_3 & \mathbf{0}_3\end{bmatrix}$ for leader measurement entries.

For follower measurement entries, the measuring agent's entry is modeled with $\mathbf{C}_L$, whereas the entry corresponding to the agent whose measurement is taken about is modeled with $-\mathbf{C}_L$. Additionally, the depth measurements taken by follower agents are modeled using the vector $\mathbf{e}_z = \begin{bmatrix} 0 & 0 & 1 & 0 & 0 & 0 \end{bmatrix}$. This is equivalent to replacing the $\bar{\mathbf{D}}_{ij}$ matrices by identity matrices, $\mathbf{I}_3$, in the the centralized observation matrix of the algorithm presented in Section IV-B.

Following the results derived in [8], the centralized gain subject to a sparsity constraint is then computed by propagating

$$\boldsymbol{\Sigma}[k+1|k] = \mathbf{A}_c \boldsymbol{\Sigma}[k|k] \mathbf{A}_c^T + \mathbf{Q}_c \tag{19}$$

and

$$\begin{aligned} \boldsymbol{\Sigma}[k+1|k+1] &= \\ &(\mathbf{I}_{6N} - \mathbf{K}[k]\mathbf{C}_c)\boldsymbol{\Sigma}[k+1|k](\mathbf{I}_{6N} - \mathbf{K}[k]\mathbf{C}_c)^T \\ &+ \mathbf{K}[k]\mathbf{R}_c\mathbf{K}[k]^T \end{aligned} \tag{20}$$

until the trace of $\boldsymbol{\Sigma}[k+1|k+1]$ reaches a steady-state value. Define $\mathbf{l}_i \in \mathbb{R}^{6N}$ as the unit vector such that all entries are zero except the i^{th} one and let $\mathbf{L}_i := \operatorname{diag}(\mathbf{l}_i)$. In the above equations, $\mathbf{Q}_c = \operatorname{diag}(\mathbf{Q}_1, \ldots, \mathbf{Q}_N)$ is the centralized process noise covariance matrix, $\mathbf{R}_c$ is the centralized observation model noise covariance matrix, and $\mathbf{K}[k]$ is given by

$$\mathbf{K}[k] = \sum_{i=1}^{6N} \mathbf{L}_i \boldsymbol{\Sigma}[k+1|k] \mathbf{C}_c^T \mathbf{M}_i \left(\mathbf{I}_{6N} - \mathbf{M}_i + \mathbf{M}_i \mathbf{S} \mathbf{M}_i\right)^{-1},$$

where $\mathbf{S} = \mathbf{C}_c \boldsymbol{\Sigma}[k+1|k]\mathbf{C}_c^T + \mathbf{R}_c$. The sparsity constraint is imposed by the matrix $\mathbf{M}_i$, which is built to encode the measurements each agent has access to. Letting $\mathbf{s}_i$ be a vector such that

$$\begin{cases} \mathbf{s}_i^j = 1 & \text{if } \mathbf{E}^{ij} = 1 \\ \mathbf{s}_i^j = 0 & \text{otherwise} \end{cases},$$

where $\mathbf{E} \in \mathbb{R}^{6N \times m}$ is the sparsity pattern matrix, with m the total measurement vector length, $\mathbf{M}_i$ is then built as $\mathbf{M}_i = \operatorname{diag}(\mathbf{s}_i)$.

Consider the vector $\mathbf{y}_{ij}(t_k) := \begin{bmatrix} \mathbf{0}_{1\times 3} & z_i(t_k) - z_j(t_k) \end{bmatrix}^T$, where z_i and z_j are the depth measurements obtained by UVs with indices i and j, respectively. Let $\boldsymbol{\Delta}_{ij}(t_k) = \mathbf{p}_i(t_k) - \mathbf{p}_j(t_k)$ and

$$\mathbf{P}_{ij}(t_k) = \begin{bmatrix} & \bar{\mathbf{D}}_{ij}(t_k) & \\ 0 & 0 & 1 \end{bmatrix},$$

with $\bar{\mathbf{D}}_{ij}$ defined as in (17). One then has that $\mathbf{P}_{ij}(t_k)\boldsymbol{\Delta}_{ij}(t_k) = \mathbf{y}_{ij}(t_k)$, from which it is possible to recover $\boldsymbol{\Delta}_{ij}(t_k)$ as

$$\boldsymbol{\Delta}_{ij}(t_k) = \left(\mathbf{P}_{ij}^T(t_k)\mathbf{P}_{ij}(t_k)\right)^{-1} \mathbf{P}_{ij}^T(t_k)\mathbf{y}_{ij}(t_k),$$

provided that $\mathbf{P}_{ij}^T(t_k)\mathbf{P}_{ij}(t_k)$ is invertible, which is the case if $z_i(t_k) - z_j(t_k) \neq 0$.

Rather than actual relative position measurements, the vector entries, $\mathbf{m}_{ij} \in \mathbb{R}^3$, of $\mathbf{m}_i$, are instead taken as

$$\begin{aligned} \mathbf{m}_{ij}[k+1] &= \alpha_{ij}\boldsymbol{\Delta}_{ij}(t_{k+1}) + \\ &(1-\alpha_{ij})\mathbf{D}_{ij}(t_{k+1})(\hat{\mathbf{p}}_i(t_{k+1}|t_k) - \hat{\mathbf{p}}_j(t_{k+1}|t_k)), \end{aligned}$$

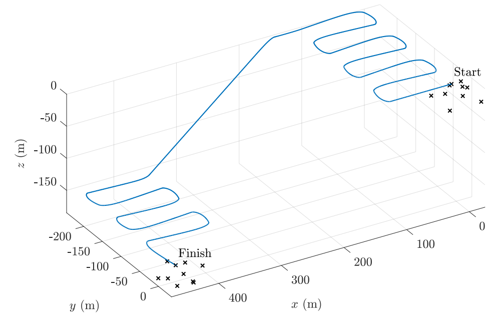

Fig. 2: Nominal trajectory of the leader agent with index 1.

with $\mathbf{D}_{ij}$ defined in (16). Each artificial relative position measurement is given by a weighted sum of the extracted position difference, $\boldsymbol{\Delta}_{ij}$, and the projection of its current prediction, $\mathbf{D}_{ij}(\hat{\mathbf{p}}_i - \hat{\mathbf{p}}_j)$, with $\hat{\mathbf{p}}_i$ and $\hat{\mathbf{p}}_j$ extracted from $\hat{\mathbf{x}}_i[k+1|k]$ and $\hat{\mathbf{x}}_j[k+1|k]$, respectively. This projection is done using $\mathbf{D}_{ij}(t_{k+1})$, which is constructed using the measured bearing angles via $\mathbf{d}_{ij}(t_{k+1})$, according to (6) and (16). Since the matrix $\mathbf{P}_{ij}^T\mathbf{P}_{ij}$ becomes close to singular if the height difference between the agents is close to zero, causing numerical instability, the weights are chosen as $\alpha_{ij} = |\mathbf{d}_{ij}^z(t_{k+1})|$. This ensures that when the extracted position difference, $\boldsymbol{\Delta}_{ij}$, is unreliable, the bearing measurement information can still be used.

V. Simulation Results

Due to space limitations, only some results pertaining to the Monte Carlo analysis are shown here.

A. Setup

The setup considered for simulation analysis consists of a set of 10 UVs performing a mission, whereby the agents must visit a set of waypoints while maintaining a certain formation. The agents start with a given spatial distribution and maintain this formation for a portion of their mission. At around $t = 400\,\text{s}$, they change to a different spatial distribution, before diving underwater, and then continue their mission.

The considered measurement topologies are presented in Figs. 3a and 3b. The agents are organized by tiers, such that $\mathcal{T}_0 = \{1, 2\} = \mathcal{V}_L$, $\mathcal{T}_1 = \{3, 4, 5, 6\}$, and $\mathcal{T}_2 = \{7, 8, 9, 10\}$ are the sets of agents in tiers 0, 1, and 2, respectively. Note that there are two leaders, agents 1 and 2, and they both are at the top of the formation, in tier 0. The cycles were made by flipping some of the edges (highlighted in green in Fig. 3b) between tiers 1 and 2 in the acyclical topology, and by introducing the blue edges around each tier of agents.

In order to evaluate the performance of the presented estimators, the algorithms were implemented on each agent and $N = 500$ runs of the mission were simulated. The root-mean-squared-error (RMSE) of the position and fluid velocity estimates, obtained for each time instant from the collection of Monte Carlo runs, was then computed, such

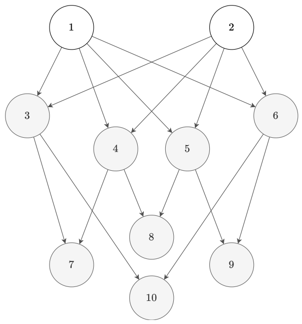

(a) Acyclical topology measurement graph.

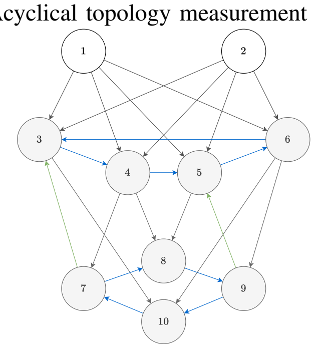

(b) Cyclical topology measurement graph.

Fig. 3: Measurement topologies.

that

$$\mathrm{RMSE}(\mathbf{x}[k]) = \sqrt{\frac{\sum_{n=1}^{N} ||\mathbf{x}[k] - \hat{\mathbf{x}}^n[k]||^2}{N}},$$

where $\mathbf{x}[k]$ is the concatenation of the state vectors of all UVs at time k, and $\hat{\mathbf{x}}^n[k]$ is its estimate obtained in the n^{th} Monte Carlo run. Additionally, in order to investigate whether the estimators are biased, the mean error of the estimated quantities, for each time instant, was computed from the collection of Monte Carlo runs, as given by

$$\mathrm{mean}(\mathbf{x}[k]) = \frac{1}{N}\sum_{n=1}^{N} \mathbf{x}[k] - \hat{\mathbf{x}}^n[k].$$

B. Results

The convergence of the algorithms was studied separately from their steady-state performance. Firstly, the convergence behavior of the presented solutions is studied. Then, the steady-state behavior is analyzed by considering small initial estimation errors.

Besides the CEKF and DEKF, the other approaches are labeled as follows. The approach presented in Section IV-A is labeled as IKF; the centralized Kalman filter approach, presented in IV-B, is labeled as CKF; and the two variants of its decentralized counterpart, presented in Section IV-C, are labeled as DKF-FCS and DKF-PCS. DKF-FCS reproduces the whole joint covariance matrix (18), whereas DKF-PCS keeps communication to a minimum and does not fill the entries corresponding to cross-covariances between neighbors of the measuring agent. Lastly, the static-gain observer presented in Section IV-D is labeled as SLTI.

TABLE I: Number of convergent runs for each EKF-based estimator.

	Acyclical	Cyclical
CEKF	443 (88.6 %)	448 (89.6 %)
DEKF	463 (92.6 %)	487 (97.4 %)

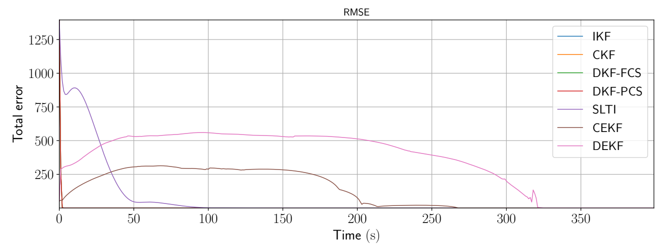

(a) Acyclical topology RMSE results of observers tuned for convergence speed.

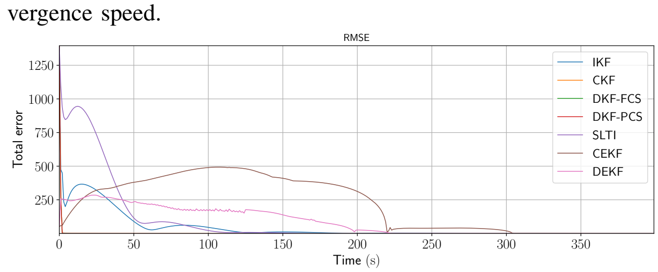

(b) Cyclical topology RMSE results of observers tuned for convergence speed.

Fig. 4: RMSE results.

1) Convergence analysis: The number of convergent runs, under each topology, for both the CEKF and DEKF, are presented in Table I. Similar results were obtained for different formation configurations and tuning parameters, and show that the centralized approach is more sensitive to initial conditions than its decentralized counterpart. As for the linear estimators, their estimates converged to the true solution on all runs. The RMSE of the convergent estimates obtained by each of the considered estimators, for both measurement topologies, is presented in Figs. 4a and 4b. Upon introduction of new edges to form cycles, the convergence speed of the IKF worsens, which is related to the fact that this observer design disregards possible cross-measurement information.

2) Steady-state performance: Here, the RMSE of the estimates obtained with each estimator, tuned for steady-state performance, is compared. The RMSE results for the acyclical topology are presented in Fig. 5a, and for the cyclical measurement topology in Fig. 5b.

From these figures, it is possible to conclude that the introduction of edges to form cycles had a beneficial effect on the performance of all estimators except the IKF and SLTI. The IKF suffers from the introduction of these edges because it lacks cross-measurement information, which leads to errors being re-introduced into the system without any kind of dampening. The SLTI, however, is impacted negatively by the presence of measurements to agents which lie on the same horizontal plane as the measuring UV. Additionally,

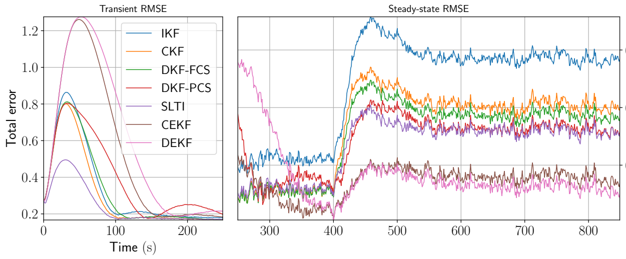

(a) Acyclical topology RMSE results of observers tuned for steady-state performance.

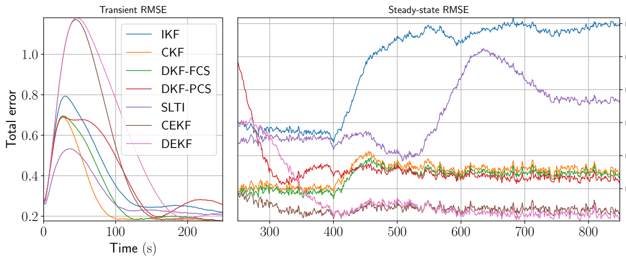

(b) Cyclical topology RMSE results of observers tuned for steady-state performance.

Fig. 5: RMSE results of algorithms tuned for steady-state performance.

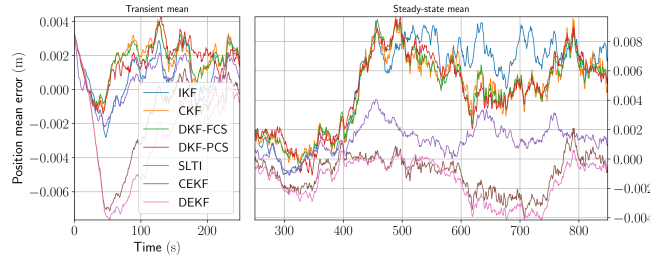

(a) Acyclical topology mean $\mathbf{p}_3^x$ estimation error of observers tuned for steady-state performance.

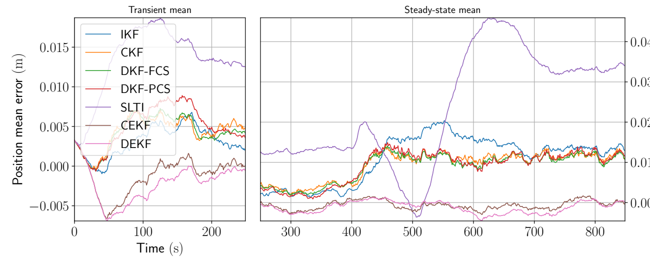

(b) Cyclical topology mean $\mathbf{p}_3^x$ estimation error of observers tuned for steady-state performance.

Fig. 6: Mean $\mathbf{p}_3^x$ estimation error of observers tuned for steady-state performance.

the centralized estimators do not provide the estimates with the lowest RMSE, which is due to the presence of a non-zero measurement error bias originating, mostly, from the construction of the direction vector in the presence of noisy bearing measurements. This measurement error bias translates into a bias in the position estimation error of the agents, which is briefly discussed in the following. For that effect, the mean results for the x coordinate of the estimated positions and fluid velocities of the UVs were investigated, and, in Figs. 6a and 6b, the results pertaining to $\mathbf{p}_3^x$ are presented. Regardless of the measurement topology, there is a clear non-zero estimation error bias for the linear estimators. Since the EKF-based approaches use the bearing angles directly (after rotation to the inertial frame), the noise affecting the measurement vector of these approaches is closer to a normally distributed noise than the one affecting the other approaches, hence there is no noticeable bias in these approaches' results, which allows them to provide better estimates.

VI. Conclusion

In this work, both centralized and decentralized cooperative navigation techniques were described and evaluated. The EKF-based approaches were compared with artificial measurement based ones, under both acyclical and cyclical measurement topologies. While the latter approaches, which are based on linear measurements, present better convergence qualities when compared to EKF-based ones, this comes at the cost of changing the noise characteristics of the measurement error vector, which prevents Kalman filter implementations from providing unbiased estimates, worsening their performance. In both the convergence and steady-state analysis of the algorithms, the decentralized approaches outperformed the centralized ones.

References

[1] P. Mendes and P. Batista, "A study on cooperative navigation of auvs based on bearing measurements," in *proceedings of Global OCEANS 2021: San Diego — Porto*, IEEE, 2021.

[2] M. F. Fallon, G. Papadopoulos, and J. J. Leonard, "A measurement distribution framework for cooperative navigation using multiple auvs," in *2010 IEEE International Conference on Robotics and Automation*, pp. 4256–4263, IEEE, 2010.

[3] A. Bahr, M. R. Walter, and J. J. Leonard, "Consistent cooperative localization," in *2009 IEEE International Conference on Robotics and Automation*, pp. 3415–3422, IEEE, 2009.

[4] L. C. Carrillo-Arce, E. D. Nerurkar, J. L. Gordillo, and S. I. Roumeliotis, "Decentralized multi-robot cooperative localization using covariance intersection," in *2013 IEEE/RSJ International Conference on Intelligent Robots and Systems*, pp. 1412–1417, IEEE, 2013.

[5] S. S. Kia, S. Rounds, and S. Martinez, "Cooperative localization for mobile agents: A recursive decentralized algorithm based on kalman-filter decoupling," *IEEE Control Systems Magazine*, vol. 36, no. 2, pp. 86–101, 2016.

[6] L. Luft, T. Schubert, S. I. Roumeliotis, and W. Burgard, "Recursive decentralized localization for multi-robot systems with asynchronous pairwise communication," *The International Journal of Robotics Research*, vol. 37, no. 10, pp. 1152–1167, 2018.

[7] D. Santos, P. Batista, P. Oliveira, and C. Silvestre, "Decentralised navigation systems for bearing-based position and velocity estimation in tiered formations," *International Journal of Systems Science*, pp. 1–22, 2021.

[8] D. Viegas, P. Batista, P. Oliveira, and C. Silvestre, "Discrete-time distributed kalman filter design for formations of autonomous vehicles," *Control Engineering Practice*, vol. 75, pp. 55–68, 2018.

[9] S. Safavi, U. A. Khan, S. Kar, and J. M. Moura, "Distributed localization: A linear theory," *Proceedings of the IEEE*, vol. 106, no. 7, pp. 1204–1223, 2018.

[10] D. Viegas, P. Batista, P. Oliveira, and C. Silvestre, "Decentralized state observers for range-based position and velocity estimation in acyclic formations with fixed topologies," *International Journal of Robust and Nonlinear Control*, vol. 26, no. 5, pp. 963–994, 2016.